

DOE/ET-53088-338

IFSR #338

**Stochastic and Collisional Diffusion in  
Two-Dimensional Periodic Flows**

*I. Doxas,\* W. Horton, and H.L. Berk*  
Institute for Fusion Studies  
The University of Texas at Austin  
Austin, Texas 78712

May 1990

*\*Department of Astrophysical, Planetary, and Atmospheric Sciences  
University of Colorado, Boulder, CO 80309*

# STOCHASTIC DIFFUSION IN TWO-DIMENSIONAL PERIODIC FLOWS

I. DOXAS

Department of Astrophysical, Planetary, and Atmospheric Sciences

University of Colorado

Boulder, CO 80309

W. HORTON and H.L. BERK

Institute for Fusion Studies

University of Texas at Austin

Austin, TX 78712

## Abstract

The global effective diffusion coefficient  $D^*$  for a two-dimensional system of convective rolls with a time dependent perturbation added, is calculated. The perturbation produces a background diffusion coefficient  $D$ , which is calculated analytically using the Menlikov-Arnold integral. This intrinsic diffusion coefficient is then enhanced by the unperturbed flow, to produce the global effective diffusion coefficient  $D^*$ , which we can calculate theoretically for a certain range of parameters. The theoretical value agrees well with numerical simulations.

The problem of diffusion of a passive tracer in a periodic two-dimensional incompressible flow has recently received considerable attention<sup>1-7</sup>. The problem is closely related to the action of turbulence on a convected field,<sup>8-11</sup> and is of interest to a wide variety of physical systems, as for instance Rayleigh-Bénard convection<sup>6</sup> and the Taylor vortices in Couette flow, various magnetohydrodynamic instabilities<sup>12</sup> and the saturated state of the ion temperature gradient driven drift wave instability<sup>13</sup>. The passive tracer has an intrinsic diffusivity  $D$ , while the global effective diffusion coefficient  $D^*$  scales, in the large Peclet limit ( $P = Lu/D \gg 1$ ) as  $D^* \sim (DLu)^{1/2}$  where  $L$  is the size of the roll and  $u$  the mean flow velocity. The  $D^{1/2}$  scaling was proposed in a related problem in reference [14], and the proportionality constant has been calculated in references [2]-[4]. Reference [2] also discussed an initial value Monte Carlo method for calculating  $D^*$  numerically. The method, which will also be used in the present work, allows an initial particle distribution to develop in time and relates the running effective diffusion coefficient  $D^*(t)$  to the second moment of the distribution. The effective diffusion coefficient  $D^*$  is then given by  $D^* = \lim_{t \rightarrow \infty} D^*(t)$ .

It is interesting to note that many hamiltonian flows lead to stochastic background diffusivity, as for instance in the problem of the drift wave instability with more than one wave<sup>13,15-16</sup>. To study this stochastic diffusion we start with a two-dimensional periodic incompressible flow described by the stream function  $\Psi = (uL/\pi) \sin(\pi x/L) \cos(\beta\pi y/L)$ . The size of the cell is  $L$ , the aspect ratio is  $\beta$ , and  $u$  is the maximum flow velocity. We choose dimensionless units such that the size of the cell is  $L = \pi$ , and the linear frequency of circulation around the O-points is  $\omega_0 = 1$ , so that  $x\pi/L \rightarrow x$ ,  $\beta y\pi/L \rightarrow \beta y$ ,  $\omega_0 t = \pi ut/L \rightarrow t$  and  $\Psi\pi/uL \rightarrow \Psi$ . In these dimensionless units the stream function becomes  $\Psi = (\sin x \cos \beta y)/\beta$ . The equations of motion of a passive tracer being advected

by the flow described by  $\Psi$  are

$$\begin{aligned}\dot{x} &= -\frac{\partial \Psi}{\partial y} = \sin x \sin \beta y \\ \dot{y} &= \frac{\partial \Psi}{\partial x} = \frac{1}{\beta} \cos x \cos \beta y\end{aligned}\tag{1a}$$

These equations can be viewed as Hamilton's equations deriving from the hamiltonian

$$H_0 = \frac{1}{\beta} \sin x \cos \beta y\tag{1b}$$

if we identify  $x \leftrightarrow p$  and  $y \leftrightarrow q$ . So the stream function for the flow is also the hamiltonian describing the motion of a pasive tracer in the flow. A phase space plot for the hamiltonian in Eq. 1b is shown in Fig. 1, for  $\beta = 1$ . The frequency of circulation around the O-point of a particle with energy  $H \ll 1$  (motion close to the separatrix) is calculated for  $\beta = 1$  in [13] and [17] and is given by

$$\omega(H) = \frac{\omega_0 \pi}{2K(m)} \approx \frac{\omega_0 \pi}{2 \ln(4/H)} \quad \text{for } H \ll 1\tag{2}$$

where  $m = 1 - H^2$  and  $K(m)$  is the complete elliptic integral of the first kind. Particles follow the streamlines around the elliptic fixed points, and are confined to one roll.

No net transport is possible in the absence of collisions in the flow described by Eqs. 1, but the flow enhances any background diffusivity so that the global effective diffusion coefficient  $D^*$  is given in terms of the background diffusion coefficient  $D$  by an asymptotic series<sup>2</sup> whose first term is

$$D^* = \frac{\sqrt{2u\beta LD}}{\pi A(\beta)}.\tag{3}$$

In the above expression,  $u$  is the maximum velocity of the flow, and  $A(\beta = 1) = 0.749$  is calculated in reference [2]. The background diffusion coefficient  $D$ , is modeled by a random walk, and is given by  $D = l^2/2\tau_k$  where  $l$  is the length of the random displacements that

produce the background diffusivity, and  $\tau_k$  the time between successive displacements. In the dimensionless units used here, Eq. 3 becomes

$$D^* = a\sqrt{D} \quad (4)$$

where  $D \rightarrow u\beta LD/\pi$ ,  $a = \sqrt{2/\pi}(1/A(\beta))$  gives back Eq. 3. In these units, the theoretical value of  $a$  for the flow described by Eqs. 1 for  $\beta = 1$ , is  $a = 1.06$ . The expansion is a good approximation to the global effective diffusion coefficient for large Peclet number ( $P = uL/D \gg 1$ ), and for small kick length<sup>2</sup>. Here we add a time dependent perturbation to Eqs. 1, calculate the resulting stochastic background diffusion coefficient  $D$  using the Melnikov-Arnold integral and compare the theoretical  $D^*$  with numerical results from a Monte-Carlo simulation using the initial value method. We restrict our numerical investigation to the case  $\beta = 1$ . An important point that has to be mentioned here is that, although the theory in [2] was developed with a collisional background diffusion coefficient in mind, all that is actually required is that the particles are well mixed within the cell. The mechanism by which this mixing is achieved is not important, and it can be either collisional (as assumed in [2]) or stochastic (as is the case here).

The hamiltonian we use to describe the perturbed flow is

$$H = \sin x \cos y + \epsilon \sin(kx + \theta_x) \cos(qy - \Omega t + \theta_y) \quad (5)$$

where  $\epsilon < 1$  is the amplitude of the perturbation, and  $k$  and  $q$  are the  $x$ - and  $y$ -wavenumbers of the perturbation relative to the wavenumbers of the unperturbed hamiltonian which are equal to one (cf. Eq. 1). The frequency of the perturbation is  $\Omega$ , and  $\theta_x$  and  $\theta_y$  are the relative phases of the two oscillations in the  $x$ - and  $y$ -directions. Once the perturbation is added, the system becomes stochastic<sup>13</sup> (see also [6] for a similar system). The change in the energy of a particle as it moves close to the separatrix from the vicinity of one X-point

to the next (e.g. ABC in Fig. 1) is given by

$$\begin{aligned}\Delta H &= \int_{-T/8}^{T/8} \frac{dH}{dt} dt \\ &= -\epsilon\Omega \int_{-T/8}^{T/8} \sin[kx(t) + \theta_x] \sin[qy(t) - \Omega t + \theta_y] dt\end{aligned}\tag{6}$$

where the integration is taken along the unperturbed particle trajectory  $x(t)$ ,  $y(t)$ . Approximate expressions for  $\Delta H$  exist in closed form for  $q > \Omega$  and for  $q < \Omega$ , and are given in references [16] and [18] as

$$\Delta H \approx 2\pi\epsilon \frac{(2\Omega)^q}{\Gamma(q)} e^{-\Omega\pi/2} \sin(k\pi + \theta_x) \sin\theta_y \quad \Omega > q \tag{7a}$$

$$\begin{aligned}\Delta H \approx & 2\epsilon \left[ \frac{2\Omega\pi}{\sqrt{1-R^2}} \right]^{1/2} \\ & \cos \left[ \left( \frac{\cos^{-1} R}{R} - \ln \gamma \right) \Omega - \frac{\pi}{4} \right] \sin(k\pi + \theta_x) \sin\theta_y \quad \Omega < q\end{aligned}\tag{7b}$$

where  $R = \Omega/q$  and  $\gamma = R/\sqrt{1-R^2}$ .

It was shown analytically in [15], and confirmed numerically in [16], that most of the contribution to  $\Delta H$  comes from a short interaction time of a particle's trajectory around  $y = m\pi$  at  $x = n\pi$  (point B in Fig. 1) so that we can write to first order

$$\Delta H \approx \frac{\partial H_0}{\partial x} \Delta x + \frac{\partial H_0}{\partial y} \Delta y = \cos(n\pi) \Delta x + \sin(m\pi) \Delta y = (-1)^n \Delta x. \tag{8}$$

We therefore see that the change in energy of a particle moving close to the separatrix is equivalent to a 'kick' in  $x$  of magnitude  $\Delta H$ . We then estimate the local background diffusion coefficient to be given by

$$D = \frac{\langle (\Delta H)^2 \rangle}{2\tau_c} \tag{9}$$

where  $(\Delta H)^2$  is averaged over the phase  $\theta_y$ . We estimate the characteristic kick time  $\tau_c$  by

$$\tau_c = \frac{1}{2}T(\Delta H) = \frac{2}{\omega_0} \ln \left( \frac{4}{\Delta H} \right) \quad (10)$$

i.e. half the period around the O-point of a particle that is  $\Delta H$  away from the separatrix, and therefore can cross the separatrix in one jump (cf. Eq. 2; the value of  $H$  on the separatrix is zero).

The global effective diffusion coefficient  $D^*$  is given by Eqs. 3 and 9 only if the flow is stochastic throughout the cell, so that there is good mixing of the particles in the cell. If the flow has a regular, as well as a stochastic part, we expect the global effective diffusion coefficient  $D^*$  to be enhanced by the ratio of the stochastic to the total area of phase space, so that  $D^* = D_{th}^*(A_{tot}/A_{st})$  where  $D_{th}^*$  is given by Eqs. 3, 9 and 10. The width of the stochastic layer and the ratio of stochastic to total area  $A_{st}/A_{tot}$ , is estimated by superimposing a Poincaré surface of sections plot with a contour plot of the unperturbed Hamiltonian (cf. Fig. 2), and calculating the area enclosed by each contour level numerically.

Another approximation of the theory is that we treat  $D$  in Eq. 9 as we treat a molecular diffusion coefficient in the diffusion equation. This is certainly correct qualitatively, but not necessarily quantitatively. Thus, in the empirical scaling  $D^* = aD^{1/2}$  the 1/2-power is expected, but it is surprising and pleasing that the data in Fig. 3 give  $a_{num} = 1.00 \pm 0.01$  while the theoretical value is  $a_{th} = 1.06$  (only a 6% difference).

We use a test particle code to evaluate the global effective diffusion coefficient for the perturbed system. Particles are loaded at time  $t = 0$  along the separatrix of the unperturbed system (cf. Fig. 3a) and the running effective diffusion coefficient is given as a function of time by

$$D^*(t) = \frac{1}{n} \sum_{i=1}^n \frac{\langle x_i^2 \rangle - \langle x_i \rangle^2}{2t}$$

where  $n$  is the total number of particles in the simulation. The global effective diffusion coefficient is given by

$$D^* = \lim_{t \rightarrow \infty} D^*(t)$$

For appropriate parameters, stochasticity quickly distributes particles evenly throughout phase space (cf. Fig. 3b), and the value of the running diffusion coefficient  $D^*(t)$  settles to a constant value  $D^*$ . A statistical test (the  $\chi^2$  goodness-of-fit test) is also used to determine if the particle distribution is a good fit to a gaussian, and reject the values of  $D^*(t)$  that came from a distribution with a bad fit<sup>2</sup>. The results are plotted in Fig. 4. The region of applicability of the theory ( $\Delta H < 0.05$ ) is expanded in Fig. 4b. As we see in Fig. 4a, for small enough kick length ( $\Delta H < 0.05$ , or  $\sqrt{D} < 0.012$ ) the numerical results are in good agreement with theory. For  $\Delta H > 0.05$  the theory overestimates  $D^*$ , probably by underestimating  $\tau_c$  in Eq. 9 (a large  $\Delta H$  will take us deep into the roll and will therefore overestimate the frequency of ‘kicking’; cf. Eq. 10). An interesting feature of the simulation results, not accounted for by the theory, is the significantly enhanced diffusivity for  $k = 1$  ( $k$  is the x-wavenumber), while all cases with  $k > 1$  are in much better agreement with theory. This enhanced diffusivity may be due to a long range correlation effect ( $k = 1$  means that the perturbation has the same x-wavenumber as the main wave). Fig. 4c finally, shows a plot of  $D^*$  against  $\sqrt{D}$  for the  $k \neq 1$  cases for the range of applicability of the theory,  $\Delta H < 0.05$ . The solid line is the least-squares fit to the data.

Recent analysis<sup>19</sup> that takes into account the fractal properties of the long trajectories along the separatrix ( $\Delta H \rightarrow 0$ ) using percolation theory, gives a new scaling law,  $D^* \sim uL(D/uL)^{3/13}$ , which arises from fractal particle trajectories with average length  $L(uL/D)^{4/13}$ . We found some correlation between this scaling law and our numerical data for  $\sqrt{D} > 0.012$  (where the present theory overestimates  $D^*$ ) but more work is needed for a more definite statement.



We have therefore demonstrated that even in the absence of a collisional background diffusivity, the system can exhibit behaviour very similar to a collisional system (the particle distribution functions are good gaussians, and we get a well defined diffusion coefficient). Furthermore, the resemblance is more than phenomenological, since, at least for a certain range of parameters, we can model the effective global diffusion coefficient by small ‘kicks’ the particle receives as it moves close to the separatrix. It should also be noted that, although the choice of perturbation in the present work was motivated by the study of the saturated state of the ion temperature gradient driven drift wave instability<sup>13</sup>, the qualitative results are more general, due to the universal aspects of the stochastic transport produced by separatrix crossing (see eg. [18], [20]-[23]). The scaling of the diffusion coefficient predicted here for instance ( $D^* \sim \epsilon$ , cf. Eqs. (4), (7) and (9)) was observed experimentally for Rayleigh-Bénard convection in reference [6], and numerically for Taylor-Couette flow in reference [5].

This work supported by US Department of Energy Grant number DE-FG05-80ET53088.

## FIGURE CAPTIONS

- Fig. 1 The phase space for the unperturbed hamiltonian.
- Fig. 2 A Poincaré surface of sections plot, superimposed on a contour plot of the unperturbed hamiltonian. We can estimate the area of the stochastic part of phase space by numerically evaluating the area enclosed by each contour.
- Fig. 3 Poincaré surface of section plots for the full hamiltonian. a) At  $t = 0$  particles are loaded along the separatrix of the unperturbed system. b) At a later time, global stochasticity sets in.
- Fig. 4 a) The stochastic global effective diffusion coefficient  $D^*$  plotted against  $\sqrt{D}$ . The range of applicability of the theory ( $\Delta H < 0.05$ ,  $\sqrt{D} < 0.012$ ) is expanded in (b). c) Plot of  $D^*$  against  $\sqrt{D}$  for the  $k \neq 1$  cases for the range of applicability of the theory ( $\Delta H < 0.05$ ,  $\sqrt{D} < 0.012$ ). The solid line is the least-squares fit to the data. The perturbation amplitude is in the range  $0.05 \leq \epsilon \leq 0.30$ .

## REFERENCES

1. H. K. Moffatt, Rep. Prog. Phys. 46, 621, 1983.
2. M. N. Rosenbluth, H. L. Berk, I. Doxas, and W. Horton, Phys. Fluids 30, 2636, 1987.
3. F. W. Perkins and E. G. Zweibel, Phys. Fluids 30, 1079, 1987.
4. B. Shraiman, Phys. Rev. A 36, 261, 1987.
5. D. S. Broomhead and S. C. Ryrie, Nonlinearity 1, 409, 1988.
6. T. H. Solomon and J. P. Gollub, Phys. Rev. A 38, 6280, 1988.
7. W. Young, A. Pumir, and Y. Pomeau, Phys. Fluids A 1, 462, 1989.
8. G. O. Roberts, Phil. Trans. R. Soc. A 266, 535, 1970.
9. G. O. Roberts, Phil. Trans. R. Soc. A 271, 411, 1972.
10. S. Childress, J. Math. Phys. 11, 3063, 1970.
11. S. Childress, Phys. Earth Planet. Interiors 20, 172, 1979.
12. W. Horton, in Handbook of Plasma Physics II, M. N. Rosenbluth and R. Z. Sagdeev ed., pp. 384-402, North-Holland, Amsterdam, 1984.
13. W. Horton, Plasma Physics 23, 1107, 1981.
14. M. R. E. Proctor, Doctoral Dissertation, University of Cambridge, 1975.
15. W. Horton, Plasma Phys. and Controlled Fusion 27, 937, 1985.
16. I. Doxas, Doctoral Dissertation, University of Texas, 1988.
17. N. O. Weiss, Proc. R. Soc. A 293, 310, 1966.
18. B. V. Chirikov, Physics Reports 52, 263, 1979.
19. A. V. Gruzinov, M. B. Isichenko and J. L. Kalda, Zh. Eksp. Teor. Fiz. (Sov. JETP) 97, 476, 1990.
20. J. R. Cary, D. F. Escande and J. L. Tennyson, Phys. Rev. A 34, 4256, 1986.
21. D. F. Escande, Phys. Rep. 121, 167, 1985.
22. D. F. Escande, in Hamiltonian Dynamical Systems, R. S. MacKay and J. D. Meiss ed., Adam Hilger, Bristol, 1987.

23. D. L. Bruhwiler and J. R. Cary, *Physica D* 40, 265, 1989.

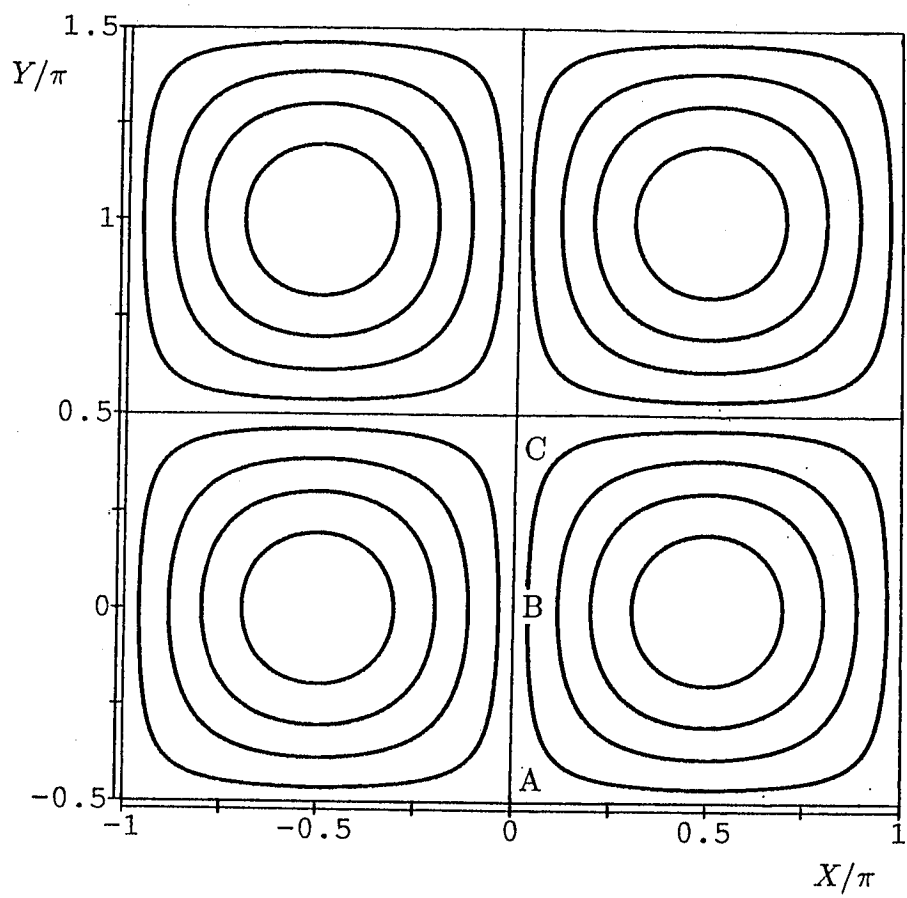


Figure 1

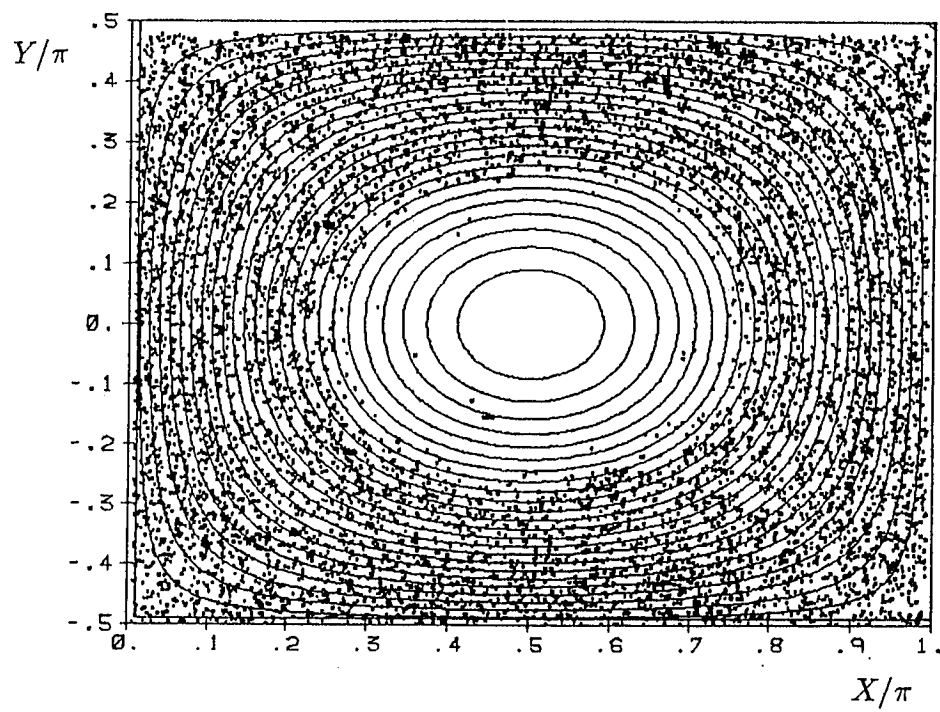


Figure 2

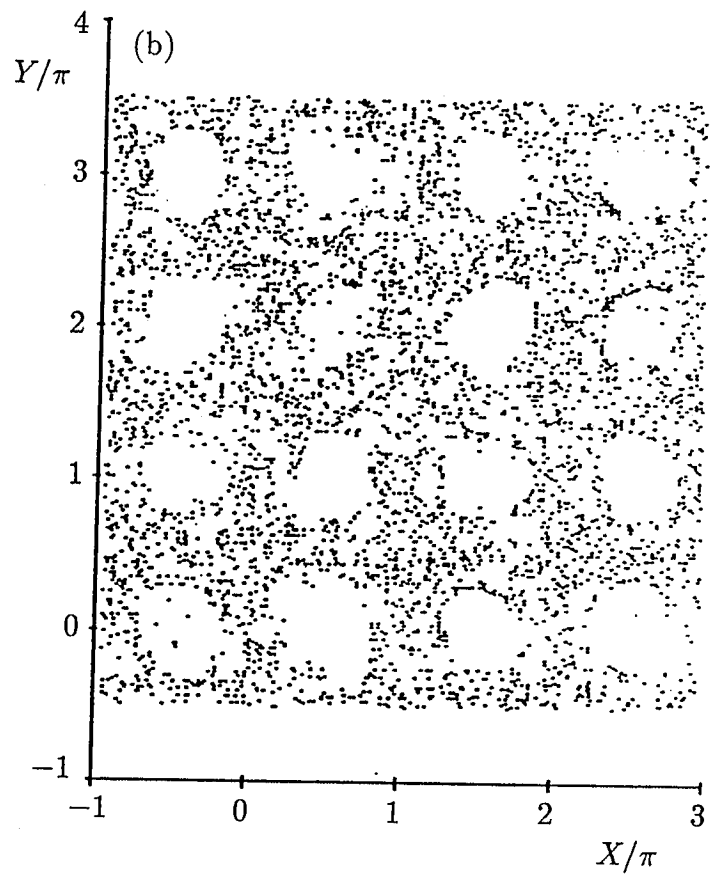
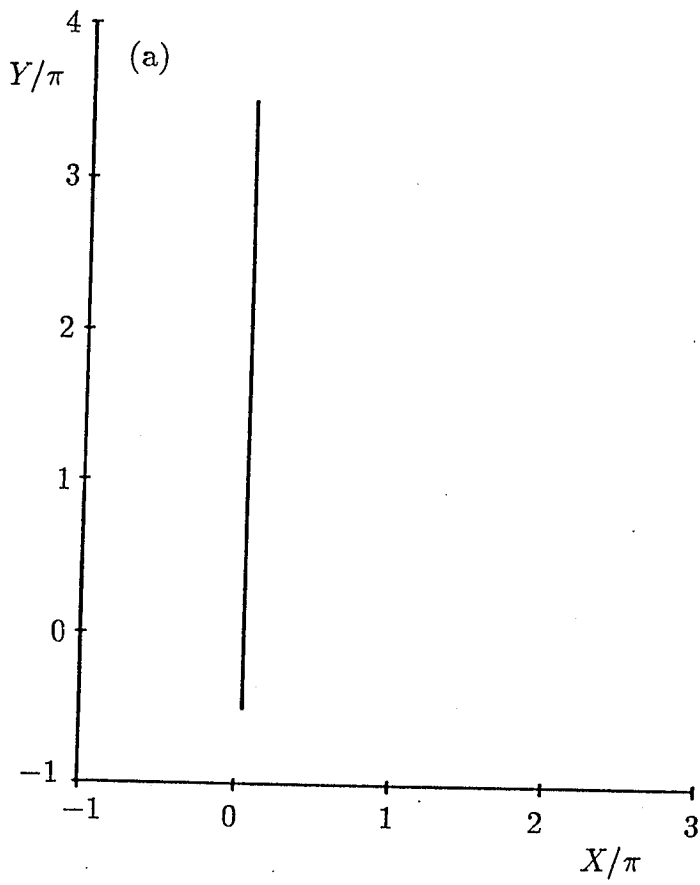


Figure 3

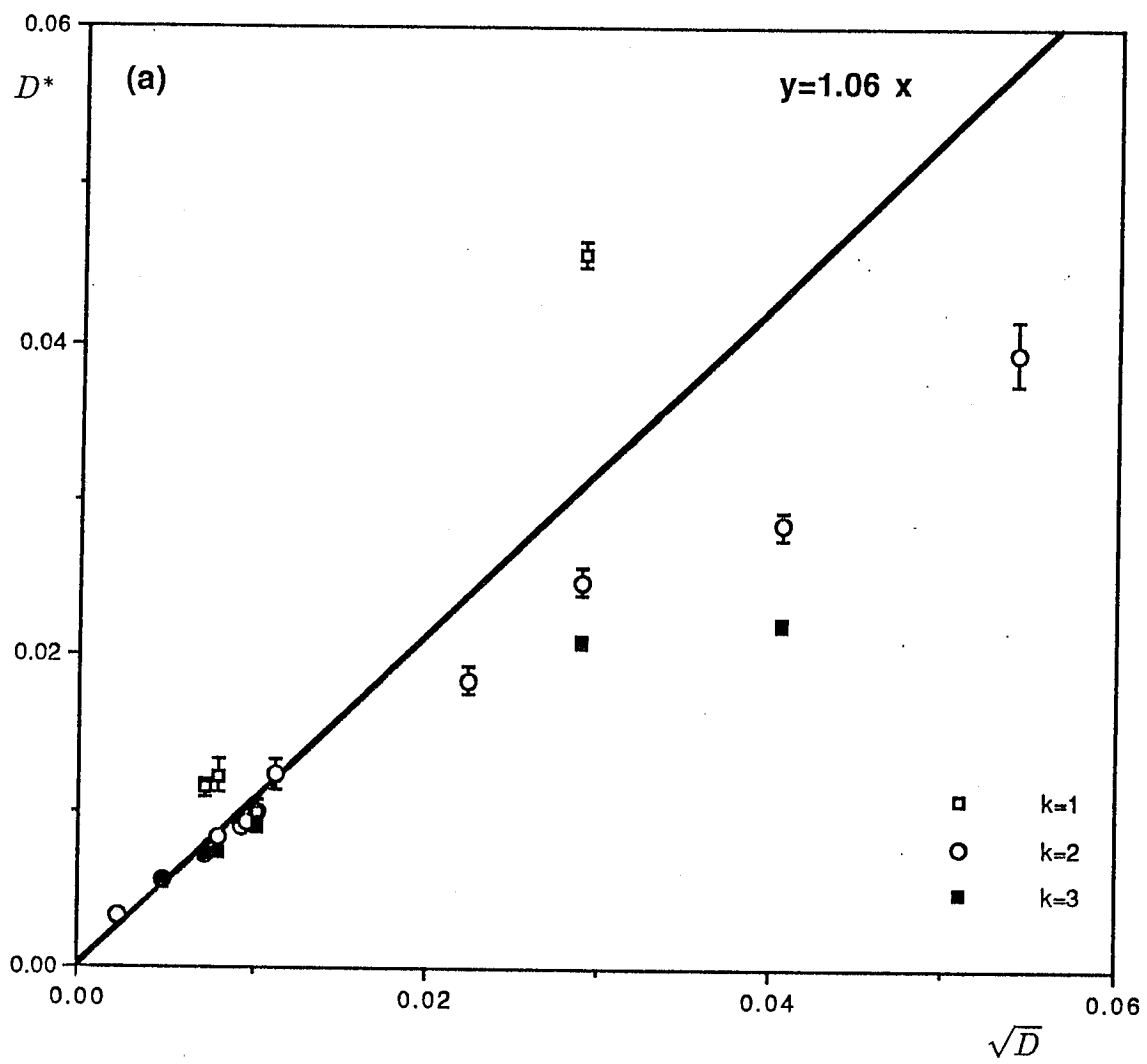


Figure 4a



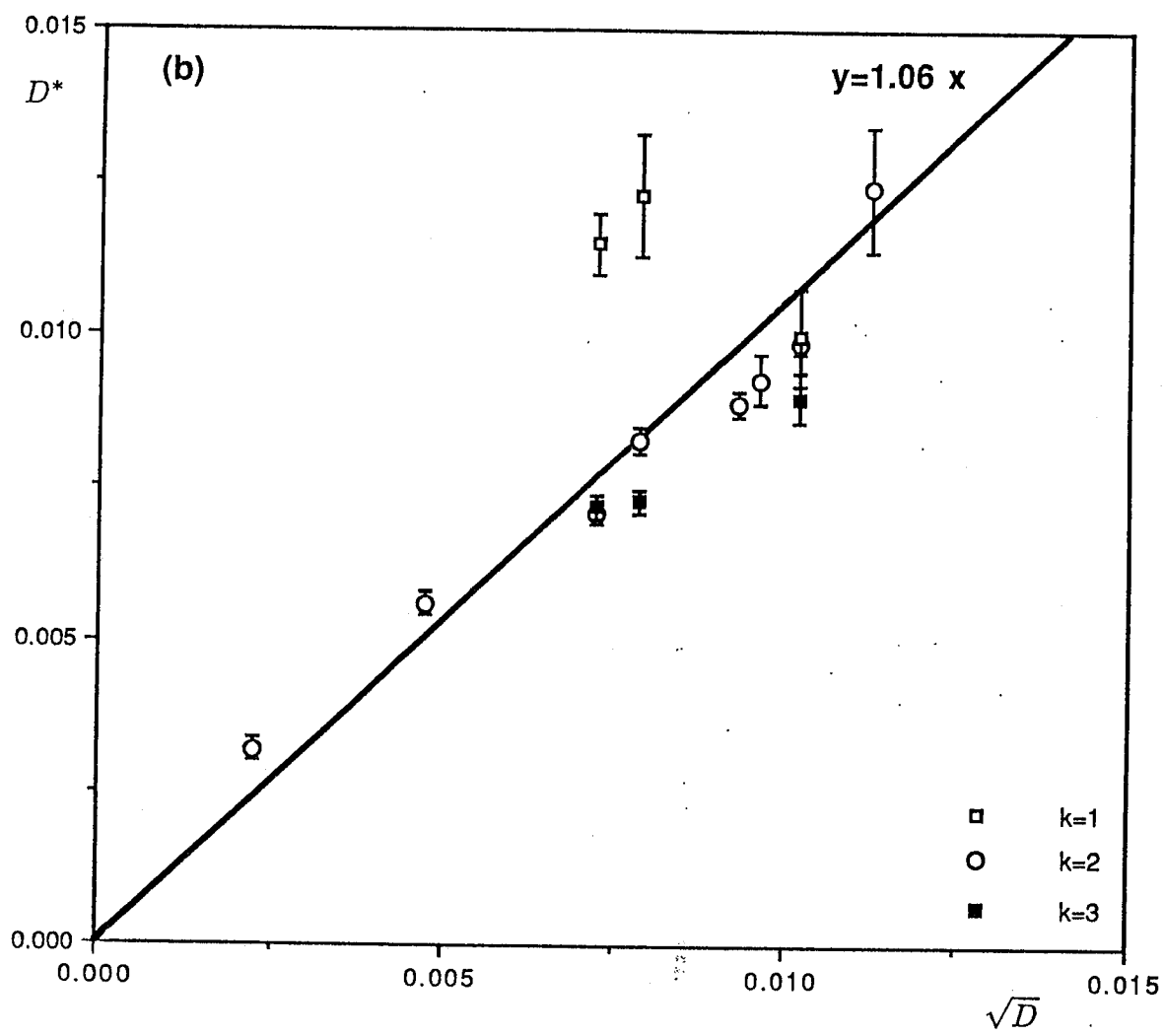


Figure 4b

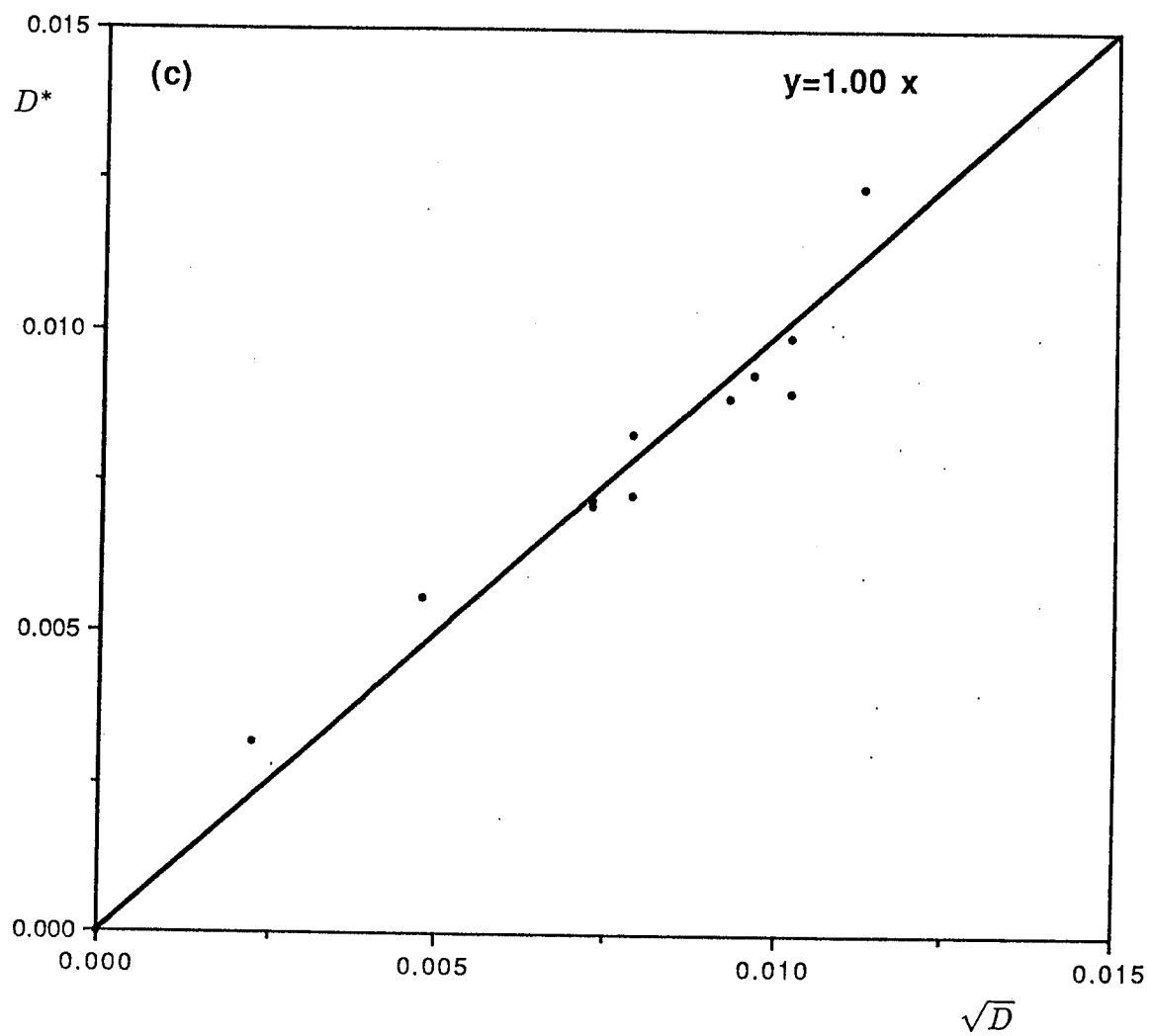


Figure 4c